Eur Spine J (2016) 25:2975–2983
DOI 10.1007/s00586-016-4570-9

ORIGINAL ARTICLE

Spinal shape modulation in a porcine model by a highly flexible and extendable non-fusion implant system

Martijn Wessels[1] · Edsko E. G. Hekman[1] · Moyo C. Kruyt[2] · René M. Castelein[2] · Jasper J. Homminga[1] · Gijsbertus J. Verkerke[1,3]

Received: 5 March 2015 / Revised: 7 April 2016 / Accepted: 14 April 2016 / Published online: 28 April 2016

Abstract
Purpose In vivo evaluation of scoliosis treatment using a novel approach in which two posterior implants are implanted: XSLAT (eXtendable implant correcting Scoliosis in LAT bending) and XSTOR (eXtendable implant correcting Scoliosis in TORsion). The highly flexible and extendable implants use only small, but continuous lateral forces (XSLAT) and torques (XSTOR), thereby allowing growth and preventing fusion.
Methods Since (idiopathic) scoliosis does not occur spontaneously in animals, the device was used to induce a spinal deformity rather than correct it. Six of each implants were tested for their ability to induce scoliotic deformations in 12 growing pigs. Each implant spanned six segments and was attached to three vertebrae using sliding anchors. Radiological and histological assessments were done throughout the 8-week study.
Results In all animals, the intended deformation was accomplished. Average Cobb angles were 19° for XSLAT and 6° for XSTOR. Average apical spinal torsion was 0° for XSLAT and 9° for XSTOR. All instrumented segments remained mobile and showed 20 % growth. Moderate degeneration of the facet joints was observed and some debris was found in the surrounding tissue.
Conclusions The approach accomplished the intended spinal deformation while allowing growth and preventing fusion.

Keywords Scoliosis · Guided growth · Non-fusion · Torsion · Animal model

✉ Martijn Wessels
m.wessels@utwente.nl

[1] Laboratory of Biomechanical Engineering, Faculty of Engineering Technology, University of Twente, PO Box 217, 7500 AE Enschede, The Netherlands

[2] Department of Orthopedics, University Medical Center Utrecht, Utrecht, The Netherlands

[3] Department of Rehabilitation Medicine, University of Groningen, University Medical Center Groningen, Groningen, The Netherlands

Introduction

Adolescent idiopathic scoliosis (AIS) is a complex three-dimensional deformity of the spine and trunk. The deformation is typically characterized by axial vertebral rotation, apical lordosis and lateral deviation of the spine and has a significant impact on patients, both mentally and physically [1, 2]. In severe cases, surgical correction and spinal fusion (spondylodesis) are required. Since the 1960s, many systems have become available and considerable technical improvements have been made [3, 4]. Besides the strategy of posterior correction and fusion, several researchers have recognized the possibility to guide the growing spine by selective tethering. This method has been shown to be effective in animal models and clinically in carefully selected patients [5, 6]. However, certain important disadvantages remain unsolved in all current systems such as loss of motion and growth arrest of the treated segments [7, 8]. Therefore, other strategies that either maintain mobility or allow growth have been explored [9, 10]. Examples are the application of tethering ligaments [11–13], growing rod systems [14, 15] and passive or motor-driven lengthening implants [16]. These strategies still have considerable limitations, e.g., not attempting to recreate normal spinal anatomy, being too stiff or requiring additional operations.

We developed a novel posterior non-fusion scoliosis correction system, referred to as the XSLATOR [17, 18]. This system applies continuous coronal and axial corrective forces. Unlike the tethering techniques used by, e.g., Braun and Schwab [12, 19], which are intrinsically similar to asymmetrical growth inhibition, the XSLATOR preserves spinal flexibility, is fully capable of growth facilitation and therefore will not inhibit growth. The system consists of two posterior implants (Fig. 1). One implant, the XSLAT (eXtendable implant correcting Scoliosis in LAT bending), is a lateral bending element, which is based on the recently developed application of shape-memory metal in posterior implants for enhanced post-operative correction [20]. The other (XSTOR; eXtendable implant correcting Scoliosis in TORsion) is a torsion-generating element that uses spinal growth for post-operative correction. Due to the flexibility of both elements, the additional stiffness to the spine is in the order of 10 % [17], which allows physiological motion. The important advantages of this are a much lower likelihood of spontaneous fusion and lower stresses on the proximal and distal anchors.

The aim of the current study is to analyze the functioning of the lateral deformation device (XSLAT) and the rotation device (XSTOR) in a growing pig model. Furthermore, the maintenance of growth, absence of fusion and soft tissue reaction will be monitored.

Methods

Study design

The devices were implanted in 12 female pigs (age 4 months, weight 55–60 kg). Six received XSLAT and six received XSTOR. In both experiments, three pigs received a wide version and three received a narrow version (Table 1). XSLAT was placed on the left side to prevent the preshaped implant from touching the spinous processes, and XSTOR was placed on the right side to mimic the corresponding placement in a potential combined application (XSLAT and XSTOR in one pig).

Devices

For both devices (XSLAT and XSTOR), we originally designed the implant to be placed fully between the pedicle screw and the spinous process (narrow version, Fig. 1a–c). This would be the least bulky design. However, as we were uncertain whether the pigs' anatomies would allow for this placement, we also designed a wide version of each implant (Fig. 1d–f). The wide version is placed partially medially, partly laterally to the pedicle screw (Fig. 1f). The mechanical behavior of both versions was similar in principle, but the narrow versions supplied slightly smaller torques (approximately, 2 vs. 2.5 Nm) [13].

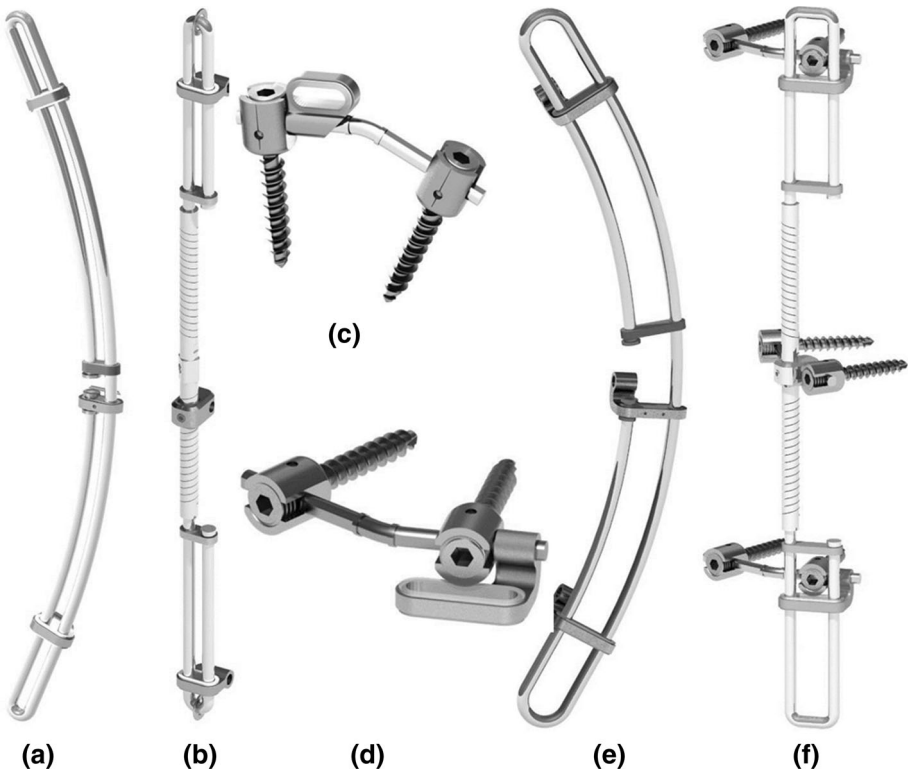

Fig. 1 XSLAT-narrow (**a**) and XSTOR-narrow (**b**) were designed to be placed between the pedicle screws using sliding anchors on a bridge (**c**). XSLAT-(**e**) and XSTOR-wide (**f**) have a slightly different design and were placed partly outside the pedicle screws (**f**, **d**)

Table 1 Implant placement

System	Pig
XSLAT	
Narrow	2, 6, 12
Wide	3, 8, 10
XSTOR	
Narrow	1, 5, 11
Wide	4, 7, 9

The lateral bending device, XSLAT, consists of a 4 mm-diameter NiTi shape-memory rod with double U-loops and three vertebral fixation parts (Fig. 2a). The system is implanted in cold condition, after which the bending moment is gradually applied as the implant warms up to the body temperature (2.8 Nm bending moment [17]). The torsion device, XSTOR, was manufactured from titanium grade 23 and consists of two torsion springs, two U-loops, and sliding anchors similar to the XSLAT (Fig. 2b). The torsion springs were preloaded (with 1 Nm torque each [17]) before fixation to the apical vertebra. For both devices, the sliding anchors are connected to the vertebrae by a transverse connector between a pair of pedicle screws (Fig. 1). The cranial and caudal anchors can slide axially over two U-shaped loops to transfer torque while still allowing growth and motion. Each implant allows about 35 % axial growth until a ring, at the end of the loops, prevents detachment of the bearings (Fig. 2b).

Animal model

Because no animal models with genuine scoliotic deformation were available, we used an inverse approach by inducing a scoliotic curve [21]. We used the growing pig model, because its biomechanical behavior and geometrical dimensions are similar to those of humans [22, 23].

Surgery

After anesthesia, the pigs were placed in prone position. Pedicle screw insertion was via the transmuscular approach to minimize soft tissue injury and disturbance of the periosteum [24]. Two pedicle screws were placed in each of the vertebrae T12, T15 and L2 and connected with a 3.5 mm-thick transverse bridge. The sliding anchor containing the implant was then connected to these bridges in a subfascial manner without tension. XSLAT was tensioned by warming to body temperature, whereas XSTOR was tensioned to apply a torque of approximately 2 Nm in the clockwise direction (as commonly seen in idiopathic scoliosis) on T15. After surgery, AP and lateral radiographs of the anaesthetized pigs were taken (Fig. 3). There were no postoperative restrictions and pain relief was given with buprenorphine.

Post-operative follow-up

The pigs were checked daily for signals of pain, mobility and progress of recovery. After 8 weeks, the pigs were

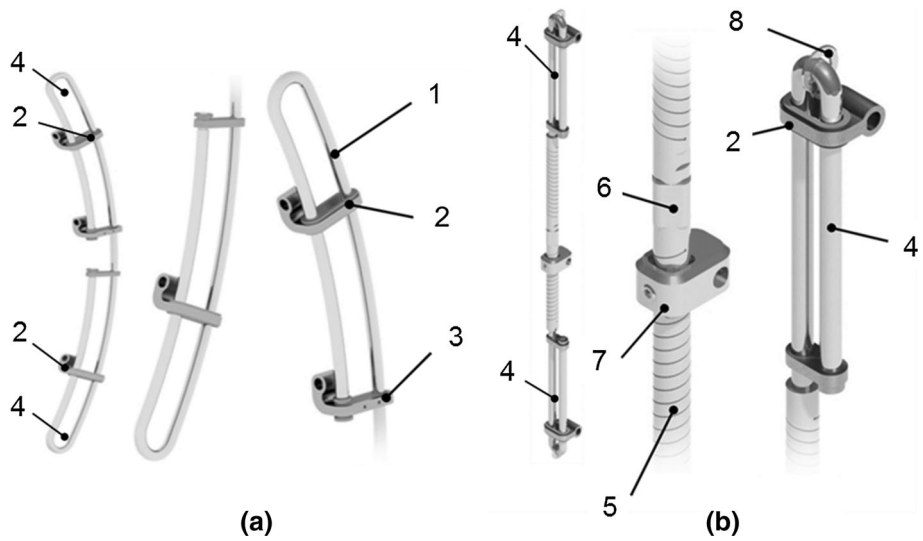

Fig. 2 **a** The XSLAT is composed of a ∅ 4 mm NiTi rod (1), two Ti6Al4V bearing systems (2) with the ability to slide (using UHMWPE bushings) over the loops and a central part (3). **b** The XSTOR (material: Ti6Al4 V) consists of two U-loops (4), two torsion springs (5), and two sliding bearing systems (2), also using UHMWPE bushings. At the center of the implant, torsion is generated by twisting, and subsequently mounting the *square* part (6) into the square hole of a box-shaped center part (7). Fixation to the spine is through transverse bridges connected to the pedicle screws. A ring (8) at the end of the U-loop prevents the bearing from being detached

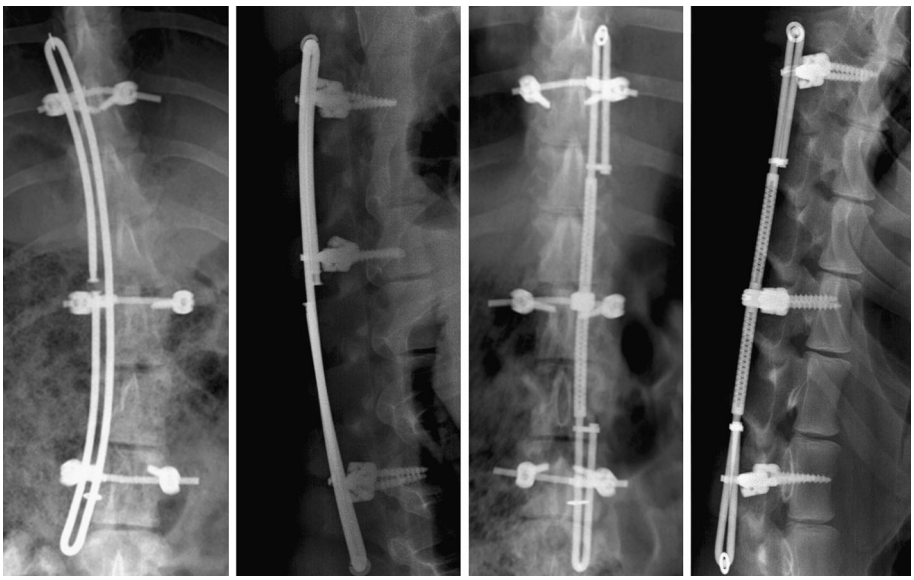

Fig. 3 Anteroposterior and lateral radiographs of the implanted narrow version of XSLAT (*left*) and XSTOR (*right*)

killed except for one randomly chosen pig from the XSTOR (wide) and one from the XSLAT (wide) group. These two were followed until 12 weeks to get more insight into the continuation of growth. Segmental growth was determined from radiographs taken of anaesthetized animals at 0, 1, 4 and 8 weeks (and 12 weeks instead of 8 weeks for the mentioned two pigs) by measuring the distance between the superior (proximal) and inferior (distal) endplates of the instrumented vertebrae. Lateral deformation and kyphosis angle of the instrumented segment were measured from the frontal and sagittal radiographs.

CT analysis

The spines were harvested en bloc and kept at 38 °C to maintain the lateral bending moment until a CT scan was made. The CT scan was examined for signs of material failure, spontaneous fusion and reactive bone formation. From T12, T15 and L2, a transverse CT slice (0.6 mm thickness) was selected at the level of the pedicle screws. The relative axial rotation angles of the vertebrae were determined by comparing manually drawn anteroposterior lines of symmetry of each vertebra. The final lateral and sagittal deformation were quantified by determining the Cobb angle and kyphosis angle between the endplates of the instrumented vertebrae T12 and L2. The lateral wedge deformation of all vertebrae within the implanted area was determined by measuring the angle between the manually drawn lines across the endplates in a frontal view.

Histology

After the CT scans, the implants were removed and checked for failure and signs of wear. Additionally, deformation of the implant, indicating a loss of functionality, was checked. The spine was manually tested for mobility before fixation in formaldehyde (4 %). Tissue reaction and presence of wear particles were examined on soft tissue samples that were collected from areas adjacent to the hardware. These were embedded in paraffin, cut into 5 μm slices and stained with toluidine blue (1 %) and hematoxylin & eosin. Control samples were taken from a location outside the area of implantation. Facet joints from vertebrae inside and outside the implanted region were harvested, decalcified with propylene diamine tetraacetic acid and embedded in a glycol methacrylate resin. Slices (3 μm) were stained with toluidine blue. These joints were categorized into three groups: adjacent to the screws (I: instrumented, $n = 61$), within the instrumented area (U: un-instrumented, $n = 19$) and outside the area of surgery (C: control, $n = 3$). Two blinded examiners classified the joint cartilage quality according to the Mankin scale (0–13) [25].

Statistical analysis

Differences in torsion angle between the four implanted groups were analyzed by one-way ANOVA followed by a Tukey HSD post hoc analysis. For the Cobb and kyphosis angles, a repeated measures (RM) analysis was used followed by a Tukey HSD post hoc analysis to determine

differences between the groups. Subsequently, for statistical relevance, the four groups were pooled into two groups: XSLAT and XSTOR, on which similar analysis were performed. For the Mankin scores, we examined differences between the groups (I, U and C) using multiple non-parametric Mann–Whitney (MW) tests.

Results

General

All implants remained functional and no serious complications occurred during the experiment (Table 2). The CT data showed small amounts of reactive bone around the screws (Fig. 4) without causing fusion. This was confirmed with manual testing. Some implants showed minor scratches and in two cases bushing material was either deformed or forced out of the casing. Wear signs were only visible in those cases. Although these implants showed damage, no decrease in mechanical functionality occurred. There was no evidence of growth inhibition due to failing bearings.

Measurements

Difference between groups in final torsion angle was significant ($p < 0.001$). There was a significant increase in Cobb angle and kyphosis angle within groups ($p < 0.02$). No differences were found between small and wide systems in torsion ($p > 0.256$), Cobb angle ($p > 0.975$) and kyphosis angle ($p > 0.858$); hence, data of wide and small versions of XSTOR and XSLAT were pooled into two groups: XSLAT and XSTOR. Difference between XSTOR and XSLAT in the final torsion angle (after 8 weeks) was significant ($p < 0.001$). Within groups, a significant increase in Cobb and kyphosis angle ($p < 0.001$) was found. Cobb angle progression was significantly different between XSLAT and XSTOR ($p < 0.001$). A significant increase in Cobb angle was measured for XSLAT

Table 2 Implant damage after explantation. No functional implant failure occurred

Pig	PE/PEEK bearings	Metal parts	Plastic deformation	Implant failure
Pig 1	One bearing deformed	Minor wear scratches	None	No
Pig 2	Bearing at apex failed	No visible damage	None	No
Pig 3	Intact	Minor wear scratches	None	No
Pig 4	One bearing failed	Wear scratches	1 bent spring	No
Pig 5	Intact	No visible damage	None	No
Pig 6	Intact	No visible damage	None	No
Pig 7	Intact	No visible damage	None	No
Pig 8	Intact	No visible damage	None	No
Pig 9	Intact	No visible damage	None	No
Pig 10	Intact	No visible damage	None	No
Pig 11	Intact	No visible damage	None	No
Pig 12	Intact	Damage at the detachment of the locking ring	None	No

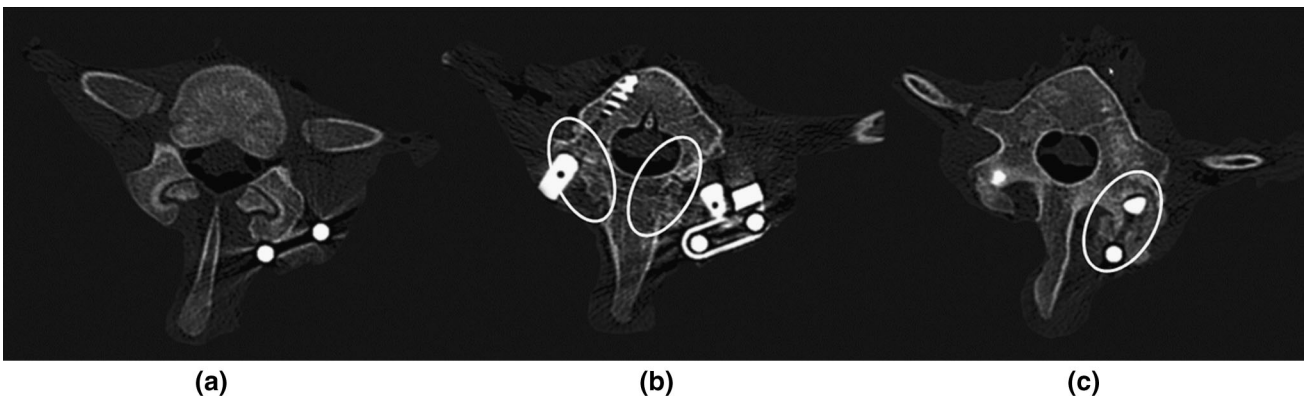

Fig. 4 Transverse CT images showing bone formation around the pedicle screws (**b**) and anchors (**c**). The vertebrae between the pedicle screw fixations showed minimal ossification (**a**)

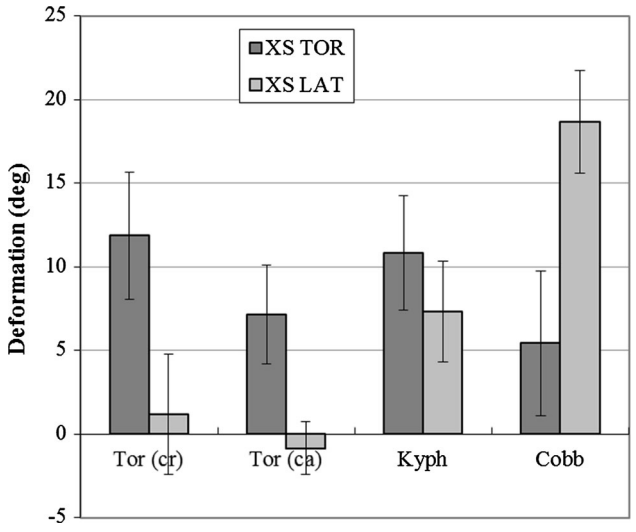

Fig. 5 *Graph* showing the induced deformation in degrees; *error bars* indicate the standard deviation. The XSTOR created torsion, both by the first spring in the three segments T12–T15 cranially [Tor (cr)] and by the second spring in the two segments T15–L2 caudally to the apex [Tor (ca)]. XSLAT created lateral bending (Cobb angle)

($p < 0.001$ and for XSTOR ($p = 0.036$). No difference between groups in kyphosis angle progression ($p = 0.183$) and in final kyphosis angle was found ($p = 0.051$).

The initial deformations directly after preloading were small (Fig. 6). XSLAT induced a lateral deformity (Cobb angle) that increased with implantation time until it reached 18.6° (range 14°–22°) after 8 weeks (Figs. 5, 6a). XSLAT did not result in any significant torsion angle (after 8 weeks: 0.2°, range −2° to 4.5°, Fig. 5). XSLAT did result in a kyphotic angle that increased with implantation time until it reached 7.3° (range 4°–10°) after 8 weeks (Figs. 5, 6b).

XSTOR, interestingly, also induced a lateral deformity (Cobb angle) that increased with implantation time until it reached 5.4° (range 2°–11°) after 8 weeks (Figs. 5, 6a). XSTOR induced an average apical torsion angle, which after 8 weeks reached 9.5° (range 6°–13°) clockwise. In the thoracic region, the mean torsion angle was 4.0° per motion segment, while it was 3.6° per motion segment in the lumbar region. After implantation, the kyphosis angle increased (no significant difference between XSLAT and XSTOR) mainly in the first week, which appeared to stabilize in the remaining period (10.5° after 8 weeks, range 5°–14°, Fig. 6b).

In the two pigs that were followed until 12 weeks, the lateral deformation seemed to still progress between 8 and 12 weeks, since their Cobb angle progression between 4 and 12 weeks was higher than the mean progression between 4 and 8 weeks in the remaining pigs (5° vs. 2° for XSLAT and 3° vs. 1.2° for XSTOR). The sagittal profile seemed to remain constant between 8 and 12 weeks (Fig. 6a, b).

Wedging of vertebrae (in the frontal plane) was observed in all XSLAT pigs, with a maximum in the middle instrumented vertebra (3.5°, range 2°–5°). All instrumented segments showed length progression with a mean of 19.5 % after 8 weeks and 24.4 % after 12 weeks. The implants did not reach their maximal length.

Histology

Some polyethylene particles were found adjacent to the bearings. Tissue surrounding screws and bearings showed some Ti alloy particles. These particles appeared to be phagocytized.

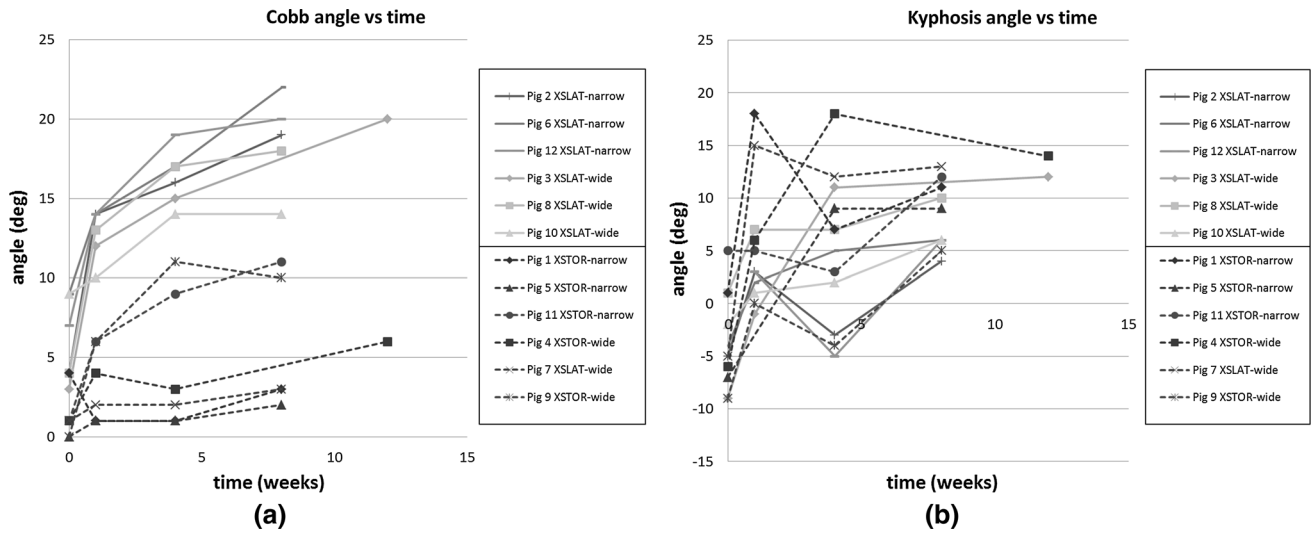

Fig. 6 **a** Cobb angles, induced by both XSLAT and XSTOR, increased during the implantation period of 8 (and 12) weeks. XSLAT induced higher lateral deformation. **b** Kyphosis increased during implantation of both XSLAT and XSTOR

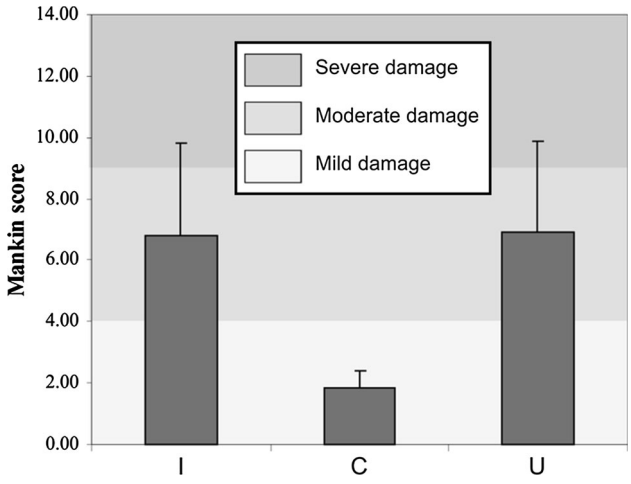

Fig. 7 The Mankin scores of the instrumented (I) and uninstrumented (U) facet joints (Mean ± SD) showed comparable values. Damage of these joints was classified as 'moderate'. The three control joints (C) showed a lower mean ($p < 0.008$), classified as 'mild'

The joints, outside the implantation area (C; control), had a Mankin score of 1.83 (range 1–3, Fig. 7). The joints at the site of fixation (I; instrumented) showed moderate cartilage damage (6.81; range 2–13, Fig. 7). The joints from sites inside the implant, but not at the fixations (U; uninstrumented), were moderately damaged (6.92, range 3–13, Fig. 7). The Mann–Whitney analysis showed no difference between U and I ($p = 0.789$); however, both U and I were statistically different ($p < 0.008$) from the control group C.

Discussion

In the current study, we have shown that both the torsional and lateral bending devices were capable of inducing a spinal deformity with similarities to (human) scoliosis. Moreover, the spines remained mobile and could elongate with growth. In contrast to the methods used by Braun and Schwab [12, 19], the devices were designed such that correction and induction of scoliosis are aimed for in a similar fashion. Whether these devices can permanently reduce a "true" scoliosis in the clinical setting remains speculative, since we induced instead of reduced a scoliosis in porcine spines that are fundamentally different in terms of geometry and loading (quadrupedal vs. bipedal). To our knowledge, there are no animal models of "true" scoliosis. Therefore, we believe that the goal of animal studies can only be modest, to merely investigate the potential to deform. Especially for our devices, where growth and mobility were important research outcomes, we preferred a healthy, untouched spine and therefore refrained from first inducing a scoliosis.

Cobb angles of XSLAT spines progressed with time, although the rate of progression declined. Undoubtedly, short-term (minutes to hours) and intermediate-term (several days) viscoelastic effects play a role in this. However, after 8 weeks, the Cobb angle induced by XSLAT was far beyond the neutral zone and the physiological ROM of porcine spines that are reported in literature [22]. Also, the apical vertebra showed a distinct wedge shape. Based on these observations, we conclude that the lateral deformation was also the result of growth adaptation as described by Hueter and Volkmann [26].

After 8 weeks, the apical torsion angle as well as the Cobb angle induced by XSTOR were far beyond the neutral zone and the physiological ROM of porcine spines that are reported in literature [22]. Although we did not investigate the effect of surgery alone, we believe that a bias due to surgery is unlikely, because the spines and pedicle entrees were always exposed on both sides of the eventual scoliotic curve. Therefore, we conclude that both the axial rotation and the lateral deformation were largely induced by the implants and mainly facilitated by adaptive tissue processes.

Growth of the spines was clearly observed. Whether this growth is comparable to the normal growth of porcine spines is unclear, as normal growth data for young porcine spines are not available from literature. If, however, the implant had hampered the spinal growth (posterior tethering), one would expect the elongation of the spines to be larger than the elongation of the implants, which was not observed. Also, posterior tethering typically results in secondary lordotic curves, which was not observed.

A moderate detrimental effect on the facet joints was found in the outer instrumented segments. This was not related to the presence of pedicle screws and therefore appears to be related to either surgical exposure of this part of the spine or less physiological mobility due to the added stiffness or pain. Only one of the 60 facet joints in the instrumented area was fused, while all others remained mobile. This is encouraging because the fast-growing porcine spine is more likely to fuse than the human spine [27]. The effect of fusionless scoliosis instrumentation on facet joints and other tissues in human and animal models has been poorly researched and still remains unclear [28, 29].

In most pigs, some bone formation was observed in the tissue surrounding the pedicle screw fixations, likely caused by damaging of the periosteum during insertion of the screws and placement of the bridges. This minor bone formation was interpreted as acceptable and may be preferable because it will consolidate the fixation anchors. In some pigs, minor bone formation was found in the tissue surrounding the implant at other locations as well. It is believed to be the result of periosteal damage caused by

implants rubbing against the spinous processes, lamina or facet joints during daily movements. Since facet and interlaminar fusions in lower animals, such as sheep, dogs, goats and pigs, are commonly achieved more easily than in humans [27, 30], we consider this minor bone formation to be acceptable.

This study has some limitations. First, we used wide and narrow versions of each implant. The use of narrow implants, which delivered slightly less lateral bending moment (for XSLAT) and torque (for XSTOR), did not seem to result in altered deformation. XSLAT-narrow created slightly larger mean Cobb angle than XSLAT-wide, while XSTOR-wide created a slightly larger mean torsion angle than XSTOR-narrow. These differences were not significant; nonetheless, this could be attributed to the small sample size.

Second, the reference X rays (day 0) were taken after the pigs spent several hours in a prone position during surgery, thereby inducing some lordosis due to the viscoelastic deformation of the spine. For the post-surgical radiographing (1, 4, 8 and 12 weeks after surgery), the time spent in the prone position was much shorter and thus less viscoelastic deformation was present. Given the flexibility of the spines postmortem (manually examined), it is most likely that this viscoelastic effect is the sole explanation for the effect of the implant on kyphosis.

The third limitation of our study is the lack of sham conditions, as the surgery itself will have an effect on the growing spine, especially in the sagittal plane. However, with respect to the intended deformations, it can be expected that this "sham" effect would be similarly present for both types of posterior implants. In fact, we did not observe any rotation in the XSLAT, and the observed lateral bending in the XSTOR where the convexity was on the implant side was actually the opposite of the curve generated by XSLAT.

Fourth, from the radiographs, accurate determination of torsion angles was not possible. For this, we used the CT analysis that was, however, only made after terminating the pigs, thus not allowing for a time-effect analysis. Visually, we did not see rotation in the animals directly after implanting the torsion device, nor on the day 0 radiographs. In conclusion, the study showed that particularly the XSTOR was capable of inducing deformities in two different planes, in accordance with the coupled motions that have been suggested previously in literature [18, 31, 32]. Our system will indirectly influence the sagittal profile by gradual reduction in the other two planes, since it has been shown in spinal motion segments that rotational, lateral and sagittal motion are coupled [18].

We believe this study can be regarded as a proof of concept of the investigated devices. Therefore, these devices may contribute to a future non-fusion approach of idiopathic scoliosis correction in humans.

In this study, we did not attempt to create a stable spine after deforming it with our inverse approach. We believe that would not yield a proper indication for creating a stable corrected spine. However, our ultimate goal is to create a stable, non-scoliotic spine. Whether the XSLATOR is capable of that will be studied in future research.

Acknowledgments This study was funded by the Technology Foundation STW, The Netherlands. We thank prof. Dr. G. Rakhorst from the Department of Biomedical Engineering and the staff from the Central Animal Facility, UMC Groningen, The Netherlands, for the accommodation and performing the surgery.

Compliance with ethical standards

Conflict of interest None of the authors has a potential conflict of interest regarding the material discussed in the manuscript.

References

1. Freidel K, Petermann F, Reichel D, Steiner A, Warschburger P, Weiss HR (2002) Quality of life in women with idiopathic scoliosis. Spine 27:E87–E91
2. Nachemson A (1979) Adult scoliosis and back pain. Spine 4:513–517
3. Kadoury S, Cheriet F, Beausejour M, Stokes IA, Parent S, Labelle H (2009) A three-dimensional retrospective analysis of the evolution of spinal instrumentation for the correction of adolescent idiopathic scoliosis. Eur Spine J Off Publ Eur Spine Soc Eur Spinal Deform Soc Eur Sect Cerv Spine Res Soc 18:23–37. doi:10.1007/s00586-008-0817-4
4. Li M, Shen Y, Gao ZL, Fang XT, Xie Y, Wang CF, Zhao YC, Zhu XD (2011) Surgical treatment of adult idiopathic scoliosis: long-term clinical radiographic outcomes. Orthopedics 34:180. doi:10.3928/01477447-20110124-14
5. Guille JT, D'Andrea LP, Betz RR (2007) Fusionless treatment of scoliosis. Orthop Clin North Am 38:541–545. doi:10.1016/j.ocl.2007.07.003
6. Crawford CH 3rd, Lenke LG (2010) Growth modulation by means of anterior tethering resulting in progressive correction of juvenile idiopathic scoliosis: a case report. J Bone Joint Surg Am 92:202–209. doi:10.2106/JBJS.H.01728
7. Tao F, Zhao Y, Wu Y, Xie Y, Li M, Lu Y, Pan F, Guo F, Li F (2010) The effect of differing spinal fusion instrumentation on the occurrence of postoperative crankshaft phenomenon in adolescent idiopathic scoliosis. J Spinal Disord Tech 23:e75–e80. doi:10.1097/BSD.0b013e3181d38f63
8. Williams GM, Klisch SM, Sah RL (2008) Bioengineering cartilage growth, maturation, and form. Pediatr Res 63:527–534. doi:10.1203/PDR.0b013e31816b4fe5
9. Maruyama T, Takeshita K (2008) Surgical treatment of scoliosis: a review of techniques currently applied. Scoliosis 3:6. doi:10.1186/1748-7161-3-6

10. Kiely PJ, Grevitt MP (2008) Recent developments in scoliosis surgery. Curr Orthopaed 22:42–47. doi:10.1016/j.cuor.2007.04.011
11. Braun JT, Ogilvie JW, Akyuz E, Brodke DS, Bachus KN (2006) Creation of an experimental idiopathic-type scoliosis in an immature goat model using a flexible posterior asymmetric tether. Spine 31:1410–1414. doi:10.1097/01.brs.0000219869.01599.6b
12. Braun JT, Hoffman M, Akyuz E, Ogilvie JW, Brodke DS, Bachus KN (2006) Mechanical modulation of vertebral growth in the fusionless treatment of progressive scoliosis in an experimental model. Spine 31:1314–1320. doi:10.1097/01.brs.0000218662.78165.b1
13. Newton PO, Fricka KB, Lee SS, Farnsworth CL, Cox TG, Mahar AT (2002) Asymmetrical flexible tethering of spine growth in an immature bovine model. Spine 27:689–693
14. White KK, Song KM, Frost N, Daines BK (2011) VEPTR growing rods for early-onset neuromuscular scoliosis: feasible and effective. Clin Orthop Relat Res 469:1335–1341. doi:10.1007/s11999-010-1749-y
15. Ouellet J (2011) Surgical technique: modern Luque trolley, a self-growing rod technique. Clin Orthop Relat Res 469:1356–1367. doi:10.1007/s11999-011-1783-4
16. Cheung KMC, Cheung JPY, Samartzis D, Mak KC, Wong YW, Cheung WY, Akbarnia BA, Luk KDK (2012) Magnetically controlled growing rods for severe spinal curvature in young children: a prospective case series. Lancet 379:1967–1974. doi:10.1016/S0140-6736(12)60112-3
17. Wessels M, Hekman EE, Verkerke GJ (2013) Mechanical behavior of a novel non-fusion scoliosis correction device. J Mech Behav Biomed Mater 27:107–114. doi:10.1016/j.jmbbm.2013.07.006
18. Meijer GJM (2011) Development of a non-fusion scoliosis correction device: numerical modelling of scoliosis correction. Dissertation, University of Twente. doi:10.3990/1.9789036532297
19. Schwab F, Patel A, Lafage V, Farcy JP (2009) A porcine model for progressive thoracic scoliosis. Spine 34:E397–E404. doi:10.1097/BRS.0b013e3181a27156
20. Newton PO, Farnsworth CL, Upasani VV, Chambers R, Yoon SH, Firkins P (2011) Dual and single memory rod construct comparison in an animal study. Spine 36:E904–E913. doi:10.1097/BRS.0b013e3181f2d10e
21. Janssen MM, de Wilde RF, Kouwenhoven JW, Castelein RM (2011) Experimental animal models in scoliosis research: a review of the literature. Spine J Off J North Am Spine Soc 11:347–358. doi:10.1016/j.spinee.2011.03.010
22. Busscher I, van der Veen AJ, van Dieen JH, Kingma I, Verkerke GJ, Veldhuizen AG (2010) In vitro biomechanical characteristics of the spine a comparison between human and porcine spinal segments. Spine 35:E35–E42. doi:10.1097/Brs.0b013e3181b21885
23. Busscher I, Ploegmakers JJ, Verkerke GJ, Veldhuizen AG (2010) Comparative anatomical dimensions of the complete human and porcine spine. Eur Spine J Off Publ Eur Spine Soc Eur Spinal Deform Soc Eur Sect Cerv Spine Res Soc 19:1104–1114. doi:10.1007/s00586-010-1326-9
24. Wiltse LL (1973) The paraspinal sacrospinalis-splitting approach to the lumbar spine. Clin Orthop Related Res 91:48–57
25. Mankin HJ, Lippiello L (1970) Biochemical and metabolic abnormalities in articular cartilage from osteo-arthritic human hips. J Bone Joint Surg Am 52:424–434
26. Stokes IA, Spence H, Aronsson DD, Kilmer N (1996) Mechanical modulation of vertebral body growth: implications for scoliosis progression. Spine 21:1162–1167
27. An YH, Friedman RJ (1999) Animal models in orthopaedic research. CRC Press, Boca Raton
28. Demirkiran G, Yilgor C, Ayvaz M, Kosemehmetoglu K, Daglioglu K, Yazici M (2014) Effects of the fusionless instrumentation on the disks and facet joints of the unfused segments: a pig model. J Pediatr Orthop 34:185–193. doi:10.1097/BPO.0b013e3182972404
29. Yilgor C, Demirkiran HG, Aritan S, Kosemehmetoglu K, Daglioglu K, Isikhan SY, Yazici M (2013) Fusionless instrumentation in growing spine and adjacent segment problems: an experimental study in immature pigs. Spine 38:2156–2164. doi:10.1097/BRS.0000000000000026
30. Pearce AI, Richards RG, Milz S, Schneider E, Pearce SG (2007) Animal models for implant biomaterial research in bone: a review. Eur Cells Mater 13:1–10
31. Sizer PS Jr, Brismee JM, Cook C (2007) Coupling behavior of the thoracic spine: a systematic review of the literature. J Manip Physiol Ther 30:390–399. doi:10.1016/j.jmpt.2007.04.009
32. Stokes IAF, Gardnermorse M (1991) Analysis of the interaction between vertebral lateral deviation and axial rotation in scoliosis. J Biomech 24:753–759. doi:10.1016/0021-9290(91)90339-O